

Article

Geochemistry and Stable Isotopes of Travertine from Jordan Valley and Dead Sea Areas

Khalil M. Ibrahim ^{1,*}, Issa M. Makhlof ¹, Ali R. El Naqah ² and Sana' M. Al-Thawabteh ¹

¹ Department of Earth and Environmental Sciences, Hashemite University, P.O. Box 150459, Zarqa 13115, Jordan; makhlof11@yahoo.com (I.M.M.); ibrahim_kh@yahoo.com (S.M.A.-T.)

² Faculty of Natural Resources and Environment, Hashemite University, P.O. Box 150459, Zarqa 13115, Jordan; elnaqa@hu.edu.jo

* Correspondence: ibrahim@hu.edu.jo; Tel.: +982-79-558-8042

Academic Editor: Antonio Simonetti

Received: 15 February 2017; Accepted: 13 May 2017; Published: 22 May 2017

Abstract: Travertine deposits in Deir Alla, Suwayma, and Az Zara areas were investigated. Mineralogy, geochemistry, stable isotopes and age dating indicate the presence of low-Mg calcite, with minor quartz components. The variable isotope ($\delta^{13}\text{C}$ and $\delta^{18}\text{O}$) signatures indicate dependence on water temperature and water/rock isotopic exchange. In contrast, the high $\delta^{13}\text{C}$ values in some travertine samples reflect $^{12}\text{CO}_2$ degassing processes, increased input of ^{13}C -enriched groundwater, and the presence of surface and groundwater hydrological systems. The high $\delta^{18}\text{O}$ values may be attributed to evaporation effects and low water temperature during the formation of localized travertine. The age of travertine is the Late Pleistocene.

Keywords: travertine; geochemistry; stable isotopes; carbon dating; Dead Sea; Jordan Valley

1. Introduction

Travertine refers to all non-marine carbonate precipitates formed at or near terrestrial springs, rivers, lakes, and caves [1], when CO_2 -rich, Ca-bearing fluids are exposed to low pressure conditions at surface conditions [2]. Travertine formation is controversial since it has been attributed to both biotic and abiotic processes [3,4]. The terms travertine and tufa are sometimes used synonymously [5]. Calcite precipitation occurs due to CO_2 -loss, and associated pH-reduction during fluid equilibration with the atmosphere [6,7]. Travertine precipitation seems to be controlled by a combination of several factors, such as: (i) a fast decrease of the hydrostatic pressure and the $p\text{CO}_2$, resulting in a rapid degassing process; and (ii) microbes and algae activity [6]. The term travertine must be retained for continental carbonates mainly composed of calcium carbonate deposits produced from non-marine, supersaturated calcium bicarbonate-rich waters, typically hydrothermal in origin [5]. Based on the CO_2 interaction with the groundwater, Pentecost [8] subdivided travertine into meteogene and thermogene deposits. CO_2 in the meteogene deposits is developed at a shallower origin, as a result of organic activity in the soil [9]. Thermogene deposits of CO_2 have a deeper origin either from magmatic degassing or from decarbonation processes [10]. Such deposits are typical of tectonically active areas where geothermal heat flux (endogenic or volcanic) is high [11]. The meteogene travertine is usually referred to as “tufa”, especially that which contains remains of micro and macrophytes, invertebrates and bacteria [11,12]. It is usually derived from lower water temperature, and lower contents of dissolved inorganic carbon (Dissolved inorganic carbon (DIC) $< 10 \text{ mmol}\cdot\text{L}^{-1}$), CO_2 partial pressure ($p\text{CO}_2 < 0.1 \text{ atm}$) and higher pH values (7–8) [10]. Meteogene usually displays low deposition rates ($< 10 \text{ mmol}\cdot\text{cm}^{-2} \text{ year}^{-1}$) and shows a negative carbon isotopic composition ($\delta^{13}\text{C}$ vs. PDB between -12 and 0‰). However, thermogene travertine displays higher deposition rates and higher ($\delta^{13}\text{C}$ vs. PDB) values [5,10]. They are characterized chiefly by high depositional rates, regular bedding

and fine lamination, low porosity, low permeability and an inorganic crystalline fabric [5]. The main distinctive characteristics of travertine and tufa are detailed in Capezzuoli et al. [5].

Travertine and tufa rocks are exposed in the eastern margins of the Dead Sea and Jordan Valley. Some investigations focused on their geotechnical properties as a decoration stone [13]. However, geochemical and mineralogical studies of such rocks are limited [14,15]. The present study aims to elucidate the mineralogy, geochemistry, stable isotope implications and age determination of the travertine and tufa formation along the eastern margins of the Dead Sea and Jordan Valley.

1.1. Location

The study area is located along the margins of the Dead Sea (Figure 1). Most of the travertine outcrops are located in the eastern Jordan Valley and the Dead Sea Transform Fault system. Three main travertine outcrops were studied including: Deir Alla, Suwayma and Az Zara (Figure 1). Representative travertine, tufa and water samples were collected from these areas.

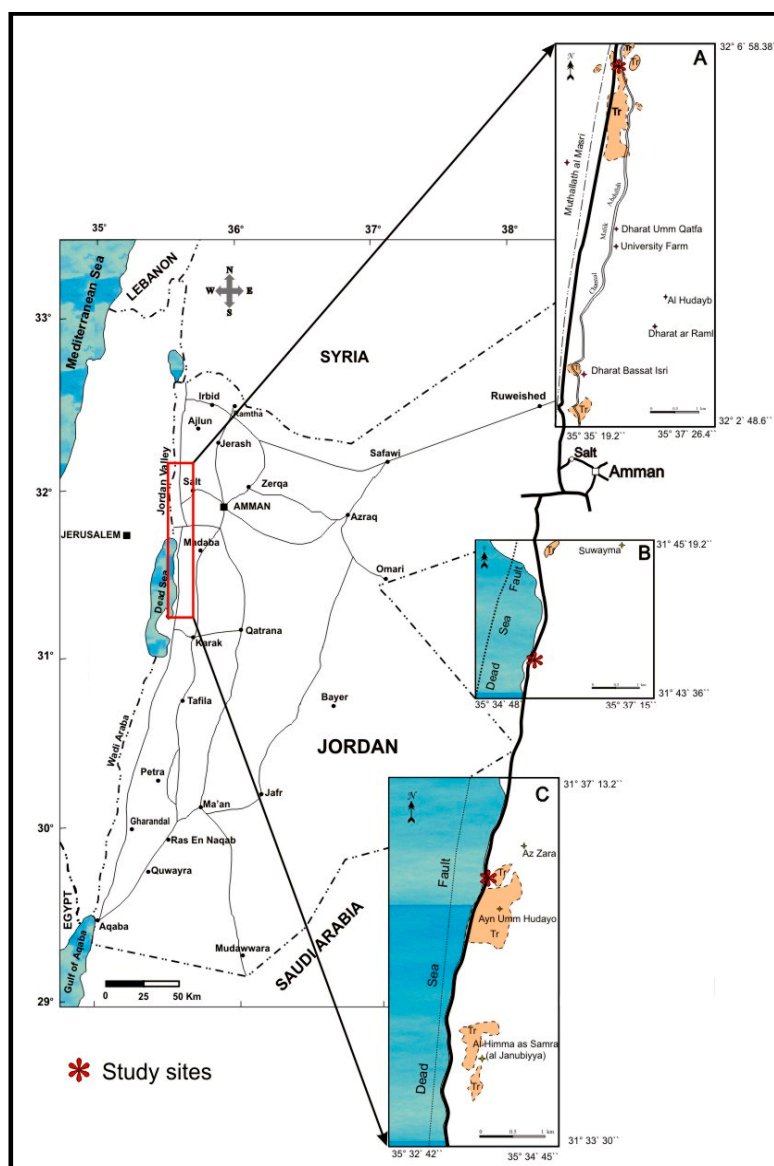


Figure 1. Location map to show the studied travertine outcrops.

1.2. Geological Setting

The travertine is exposed in a highly tectonized area associated with the main Dead Sea Transform Fault (Figure 2). It is an 1100 km long sinistral fault system that connects the Gulf of Aqaba-Red Sea spreading system to the convergence zone of the Taurus–Zagros Mountains [16]. This fault is a left lateral transform plate boundary, separating the Arabian plate in the east and the Palestine-Sinai sub plate (part of the African plate) in the west [17]. It has been active since ca. 13–18 Ma ago with movement continuing today [17,18]. Most of the faults in the study area are related to the stress fields associated with the transform boundary.

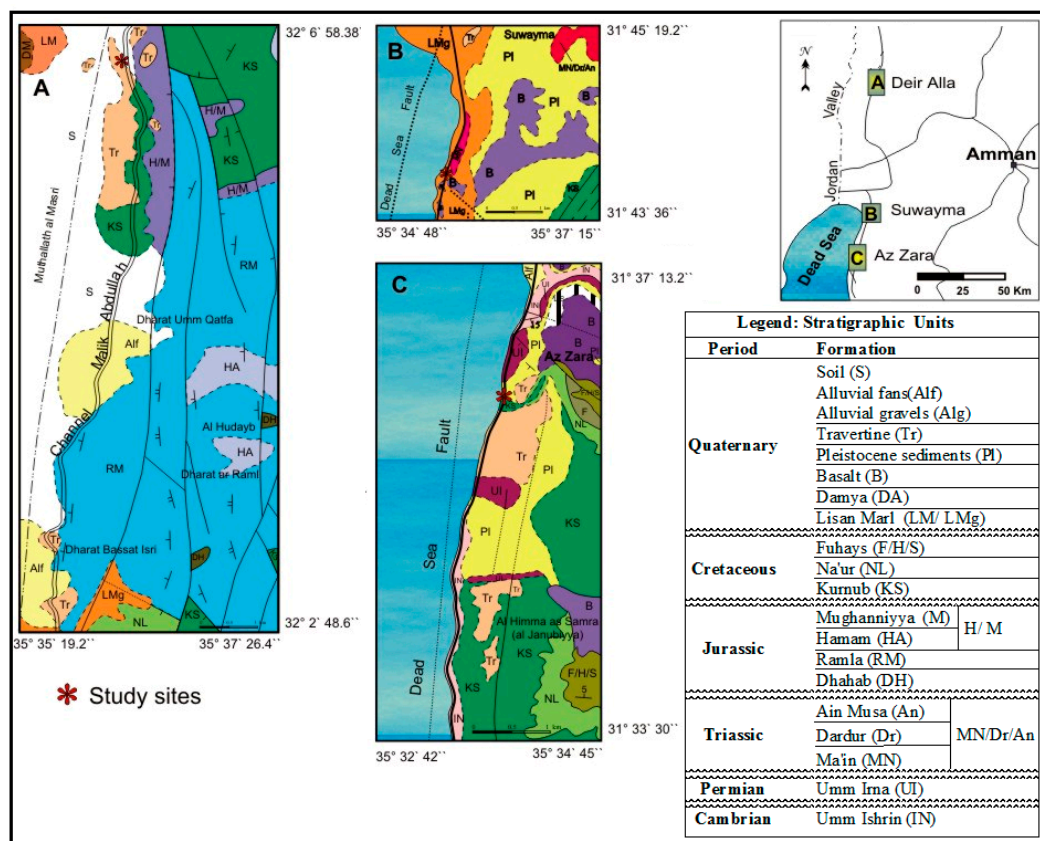


Figure 2. Geological maps of the studied travertine outcrops.

The stratigraphic sequence in the studied areas, as illustrated in the simplified geological maps in Figure 2, comprises a wide range of rock units including Cambrian, Permian, Triassic, Jurassic and Cretaceous sandstones, shale and carbonates (Figure 2). Quaternary deposits occur widely in the form of marls, siltstone, basalts, travertine, fluvial and alluvial sediments.

The studied travertine facies are composed of crystalline crust, shrub, paper-thin raft, coated gas bubble, reed, lithoclasts, pebbly travertine, and palaeosols with a tufa carbonate facies of macrophyte encrustation deposits, bryophyte build-ups, biomicrites and green and grey marls (Figure 3). The Deir Alla travertine is formed in a terraced and smooth slope depositional setting, where it has been subjected to meteoric diagenesis.

The inactive thermogene Suwayma travertine is deposited in fissure-ridge and depression depositional setting, with meteoric and burial diagenetic processes [19]. Both localities are characterized by hard crystalline travertine with low organic content. Az Zara travertines were deposited under self-built channels' depositional settings. Az Zara active tufa was formed in a predominantly fluvio-palaeustrine environment, which is friable and rich in organics and clays.

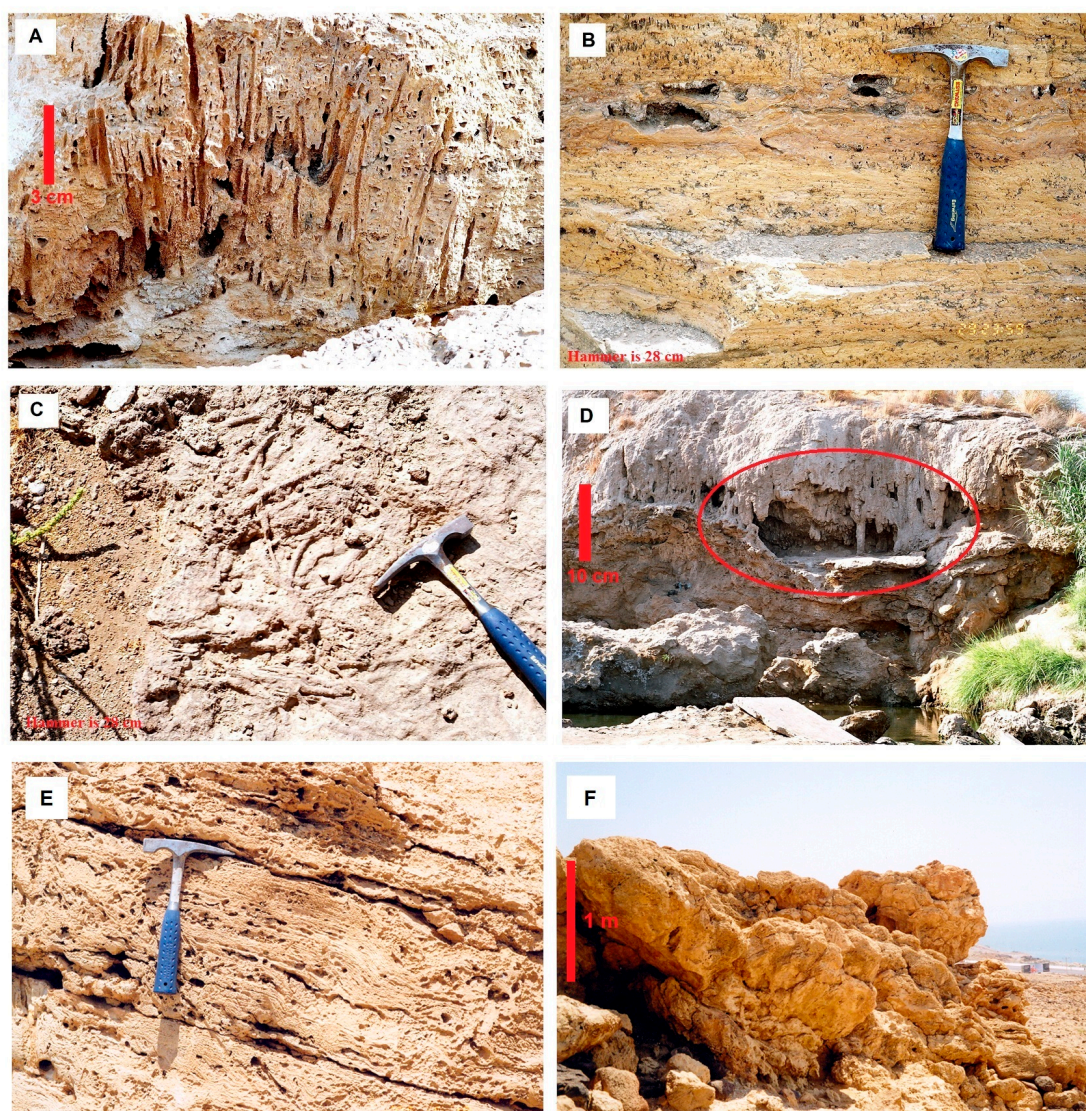


Figure 3. Selected field photos of the studied travertine: (A) root casts, downward tapering, rare lateral roots, smooth tube-like, ranging from 0.5 to 7.0 cm in length and from 0.1 to 3.5 cm in diameter preserved in porous travertine from Deir Alla; (B) tiny travertine from Deir Alla with irregular elliptical cavities are partly to completely infilled by secondary materials; (C) interconnected root traces on the upper bedding plain indicating the plants types of Az Zara area; (D) stalagmites and stalactites features (red circle), which are formed near Az Zara hot spring; (E) wavy laminae resembles stromatolite in Suwayma travertine, bedding plains indicate three stages of travertine precipitation; (F) the mound of travertine standing in an erosional relief in Suwayma. The hammer is 28 cm long.

1.3. Hydrology and Hydrogeology

The physiographic situation of the Dead Sea and Jordan Valley displays morphotectonic depressions (Figure 1). Therefore, most of the rainfall-infiltrated water emerges once again in the form of springs, and the general flow direction is due west, towards the Dead Sea and Jordan Valley. The water temperature of some springs is moderate (18–21 °C). The discharge amount is seasonal such that it increases during the winter and drops in the summer [20].

The groundwater around the Dead Sea is found in two aquifer complexes; the first is the upper limestone aquifer complex (Upper Cretaceous), and the second is the sandstone aquifer complex (Lower Cretaceous). The total amount of groundwater associated with the upper aquifer is around

87 million m³/year [20], and half of it discharges on the surface through springs. The total discharge of the lower aquifer is around 90 million m³/year, and the water is mostly thermal and mineralized [21]. The Jordan Valley floor consists of recent alluvial fan sediments inter-tonguing with Pleistocene salty, clayey sediments of the Lisan Formation. The available groundwater in this area ranges from 18–20 million m³/year [22].

Springs issued east of Deir Alla are alkaline with prevailing bicarbonate in summer, and alkaline with prevailing chlorides in winter. Fe oxides precipitate as soon as the water mixes with the Zarqa River water [23]. The number of thermal springs in Ma'in area is approximately 109, with temperature exceeding 34 °C. All such thermal springs are classified as hyperthermal [24]. Sixty-four hyperthermal springs are located in the northern part of Wadi Zarqa Ma'in forming the "Hammamt Ma'in", with 19 million m³/year total discharge into the Dead Sea. The rest of the hyperthermal springs are aligned in a north–south trend at the Az Zara area, on the eastern shore of the Dead Sea. The total discharge into the Dead Sea from the Az Zara area is 17 million m³/year [23].

2. Materials and Methods

More than 80 travertine samples were collected from three investigated areas representing both vertical and horizontal sections. The mineralogy of 18 samples was determined by X-ray diffraction (XRD), using a Phillips X' Pert Pro PW 3040/80 diffractometer (Lelweg 1, 7602, EA Almelo, The Netherlands). Twenty-two samples were selected for major and trace elements determination by X-ray fluorescence (XRF)—using a Phillips MagiX PW 2424 diffractometer (Lelweg 1, 7602, EA Almelo, The Netherlands). Radiogenic and stable isotope measurements were also carried out. The method used for $\delta^{18}\text{O}$ measurements is CO₂ equilibrium/Delta Plus XP Isotope Ratio Mass Spectrometer HDO (ThermoFisher Scientific, Walton, MA, USA) using a platinum catalyst modified from (International Atomic Energy Agency). Measurements of ¹⁴C and $\delta^{13}\text{C}$ are done by a benzene synthesis line and Liquid Scintillation Counter. The method is modified by (IAEA) technical procedure #25. The measurements of the (¹³C/¹²C) isotopes are made relative to the Vienna Pee Dee Belemnite standard (VPDB), and the water oxygen is based on a Vienna Standard Mean Ocean Water (VSMOW).

The ratios of (¹³C/¹²C) and (¹⁸O/¹⁶O) are expressed in the δ notation. The values of $\delta^{18}\text{O}$ are interchangeable according to such equations [8]: $\delta^{18}\text{O}$ (VSMOW) = [1.03088 $\delta^{18}\text{O}$ (VPDB) + 30.88] and $\delta^{18}\text{O}$ (VPDB) = [0.97008 $\delta^{18}\text{O}$ (VSMOW) – 29.94].

The calculation of travertine age was performed by the equation set by Vogel [25] and used by Thorpe et al. [26]. The decay rate constant (λ) is assumed to equal 1.209×10^{-4} year⁻¹. The value dilution factor is 0.85 ± 0.05 [8,26].

3. Results and Discussion

Petrographic investigation reported the presence of eight travertine and four tufa lithofacies in the studied sites. The description of these lithofacies is summarized in Table 1.

Table 1. Summary of travertine and tufa lithofacies in the studied travertine outcrops.

Locality	Lithofacies	Description
Deir Alla & Suwayma Travertine	Crystalline crust	Dense, crudely fibrous, elongated calcite crystals (ray crystals)
	Shrub	Small bush-like growths, on horizontal-semi-horizontal surfaces
	Rafts	Thin, delicate and brittle crystalline layers
	Lithoclast	Penecontemporaneous, angular to subangular travertine fragments in different size, formed by erosion of the upper slope and collapse of waterfalls and terrace cliffs
	Coated gas bubble	Gas bubbles are coated by rapid precipitation of calcium carbonate

Table 1. Cont.

Locality	Lithofacies	Description
Deir Alla & Suwayma Travertine	Reed	Rich in molds of reed and coarse grass
	Pebbly	Rounded pebbles of limestone, chert and basalt
	Palaeosol	Exposure of travertine surface to rainwater, subaerial desiccation, and biological activities associated with soil formation
Az Zara Tufa	Macrophyte encrustation	Calcified stems, twigs and leaves that represent rushes, reeds and unidentifiable bushes.
	Bryophyte build-ups	Laminated deposits that commonly form asymmetrical mounds or small domes, up to 1.75 m thick or stacked sequences up to 2 m high.
	Biomicroites	Tabular layers, tens of centimeters thick, mostly at the top of the tufa succession. They consist of massive biomicroites or, in some places, biosparites.
	Marls	Massive lenticular beds that are associated with macrophyte palisades. They contain plant debris.

3.1. Mineralogy

Semiquantitative determination of mineral phases was reported by the X-ray diffraction. In the present work, components other than calcium carbonate may be defined as accessories. X-ray diffraction of travertine from Deir Alla, Suwayma, and Az Zara indicates close similarity. They are predominantly composed of calcite (Figure 4). Deir Alla and Suwayma samples occasionally contain a very low percent of quartz and Fe-oxides. Sample (D26a) shows a frequent amount of aragonite (Figure 4). Traces of gypsum, dolomite and halite may also occur.

Petrographic study by Al-Thawabteh [19] indicated that most of the Fe present in travertine and tufa is autochthonous, i.e., formed or grown in situ and has not been transported. Precipitation of hydrated Fe-oxides occurs when groundwater containing ferrous ions encounters the atmosphere. In contrast, quartz enters the travertine realm as a detrital mineral, derived from the soil and bedrocks, and are therefore considered as allochthonous minerals.

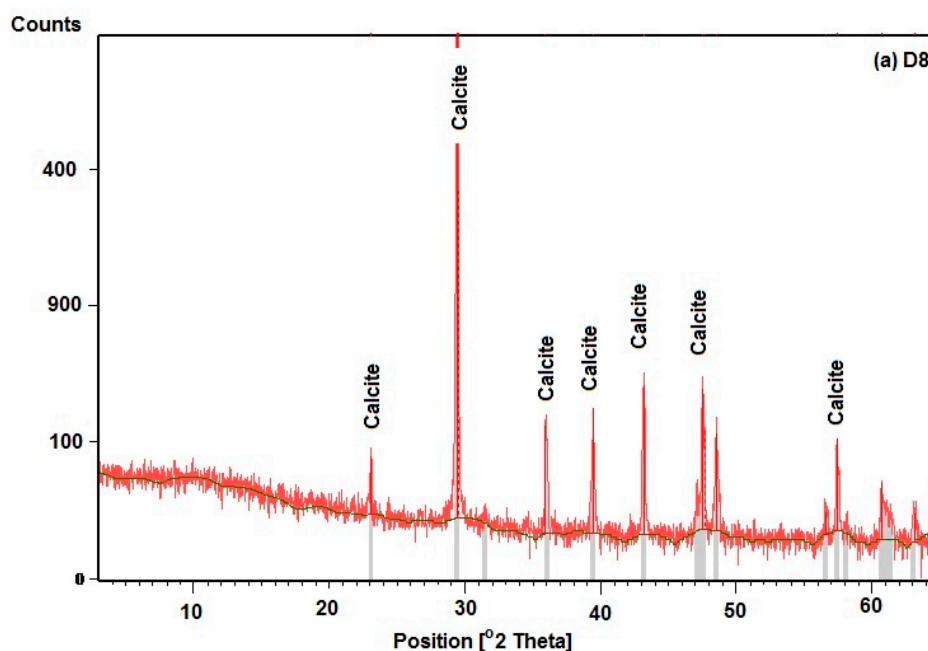


Figure 4. Cont.

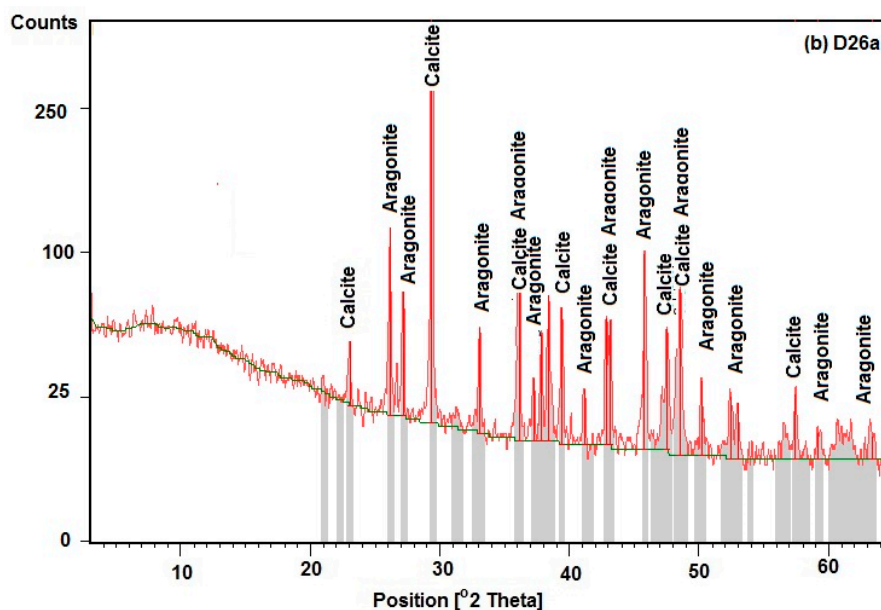


Figure 4. Selected X-ray diffractograms of the studied travertines (a) D8, (b) D26a.

Calculations of the theoretical mineralogical composition including $MgCO_3$ percent are presented in Table 2. In Deir Alla, the detrital quartz grains are rare compared to Suwayma and Az Zara (Table 2). It is believed that they are derived from sandstone when hot groundwater emerges onto the surface. In addition, Deir Alla travertine includes different types of clay minerals that vary from 0.19–1.47 wt % (Table 2). In thermogene travertine of Suwayma and Az Zara, the presence of clay (2.82 wt % and 0.85 wt %, respectively) may be due to the hydrothermal alteration of the host rock.

Table 2. Calculated theoretical mineralogical composition of travertine and tufa samples (wt %).

No.	D3	D8	D11	D18	D23b	D26a	D26b	D29		
Clay	0.8	0.7	0.4	1.5	0.4	0.7	1.3	0.2		
Dol	0.5	0.7	0.5	0.7	0.4	0.9	0.5	0.4		
Cc	98.4	94.3	97.2	93.0	94.3	93.7	98.5	98.8		
Qz	nd	nd	nd	0.1	0.1	0.1	nd	nd		
Mgs	0.4	0.4	0.3	0.5	0.3	0.8	0.4	0.3		
Others	2.4	4.3	1.8	4.7	4.8	4.4	1.8	0.7		
No.	S1d	S10	S19	S27	S32	S34	S38	S39	S45	S47b
Clay	9.2	2.2	4.5	1.4	1.2	1.8	1.8	1.3	2.2	2.8
Dol	2.1	2.3	2.7	1.3	3.0	3.4	2.0	2.2	2.5	2.9
Cc	72.0	90.7	88.9	94.4	92.3	90.7	93.8	93.1	90.7	87.8
Qz	3.7	0.5	1.5	0.2	0.4	1.1	0.4	0.3	0.9	1.2
Mgs	1.9	1.59	1.99	0.9	1.9	2.2	1.3	1.4	1.7	1.9
Others	12.9	4.0	4.4	2.7	3	3.0	2.3	2.7	3.5	5.3
No.	Z1			Z1*			Z3		Z4	
Clay	0.8			0.5			1.0		1.1	
Dol	2.5			1.8			1.5		2.2	
Cc	91.8			88.7			93.5		94.2	
Qz	0.8			1.8			0.1		0.2	
Mgs	1.8			1.1			1.0		1.4	
Others	3.9			7.1			3.7		2.1	

Z1 and Z1* are tufa samples. (nd: is not detected; D: Deir Alla; S: Suwayma; Z: Az Zara; Dol: dolomite; Cc: calcite and/or aragonite; Qz: quartz; Mgs: magnesite).

3.1.1. MgCO₃

The calculated MgCO₃ represents all of Mg in the studied travertine. The Mg is usually incorporated in the calcite, aragonite, and dolomite crystals, or it may form magnesite. In Deir Alla travertine, the calculated MgCO₃ content ranges from 0.3 wt % to 0.8 wt %, with a mean value of 0.4 wt %, whereas in Suwayma travertine, the range is from 0.9 wt % to 2.2 wt %, with an average value of 1.7%; meanwhile, the calculated MgCO₃ content of Az Zara travertine and tufa ranges from 1.0% to 1.8%, with a mean value of 1.3% (Table 2). This indicates that the calcite in such travertines and tufas is invariably of low Mg calcite [27] (Table 2). Calcite that contains less than 8% of MgCO₃ has been defined as low-Mg calcite, whereas calcite, with more than 8–11% of MgCO₃, has been defined as high-Mg calcite [27].

3.1.2. Calcium Carbonate (CaCO₃)

Deir Alla travertine consists mainly of calcium carbonate with an arithmetic average value of 95.5% (Table 2, shown as cc). According to Pentecost [8], meteogene deposits have a high average of CaCO₃ content with a median of about 92.9%, and an upper range of 99.3%. In addition, Pentecost [8] indicated that active meteogene deposits have a lower CaCO₃ content (mean 91.2%, No. of samples = 28) than their inactive meteogene counterparts (mean 94.8%, No. of samples = 22). This might be due to the loss of organic matter in the older deposits. Consequently, the Deir Alla travertine can be classified as inactive super-ambient meteogene deposits based on the CaCO₃ content [8].

The mean calcium carbonate abundance in Suwayma travertine is about 89.18% (Table 2). The CaCO₃ content of thermogene travertine is broadly similar to that of meteogene [8]. Therefore, the Suwayma travertine can be classified as thermogene deposits based on its CaCO₃ content. Az Zara travertine mainly consists of calcium carbonate with a mean of 92% (Table 2). Az Zara travertines and tufa can be classified as inactive and active thermogenic deposits, respectively. Az Zara deposits are localized and are commonly associated with regions of Quaternary basaltic outcrops and recent tectonic activities related to the Dead Sea Transform Fault System.

In general, calcium carbonates in travertine are formed of various combinations of aragonite and calcite polymorphs [28]. No attempts were carried out in this study to investigate the controls of calcium carbonate polymorph precipitation. The factors that control calcite and aragonite precipitation in travertine are still open to debate [28–31]. The precipitation has been variously attributed to water composition, water temperature, growth inhibitors (e.g., Mg/Ca ratio), and/or CO₂ degassing and saturation levels [29]. Aragonite may co-precipitate with calcite at a high CO₂ content and rapid CO₂ degassing, irrespective of the Mg/Ca ratio [30], or aragonite may precipitate from low levels of CO₂ degassing, provided the Mg/Ca ratio is high enough to inhibit calcite precipitation [30].

3.2. Geochemistry

3.2.1. CaO and MgO

The XRF results indicate that CaO wt % in the travertine ranges from 48.38% to 55.8% (Table 3). The relationship between CaO% and SiO₂% is presented in Figure 5a supported by the negative correlation coefficient of -0.82 in the correlation coefficient matrix (Figure 6). The inverse relationship between these two oxides (Figure 5a) indicates that they are involved in two different phases. A similar conclusion can be noted in Figure 5b, which exhibits the relationship between CaO and Al₂O₃.

It is evident that the studied travertine samples have low Mg content (Table 3), which is less than 1.0 wt % MgO with a mean value of 0.19 wt %. Consequently, calcites of such travertine are invariably of low Mg. The high value of Mg in some Suwayma travertine samples (Table 3) may have resulted from the input of Mg-enriched solutions that could lead to slight dolomitization; i.e., formation of diagenetic dolomite. Mg forms a solid solution series with calcite and a wide range of compositions are possible. Figure 6 shows the negative correlation between CaO and MgO, which indicates that Mg substitutes Ca in calcite crystals. Previous studies by Pentecost [8] show that a few meteogene

travertines are composed of calcite, which exceed 1% of Mg by weight, and yield a mean value of 0.29 wt %. Thermogene travertine consisting of calcite has similar Mg concentration similar meteogene travertine [8].

Table 3. X-ray Fluorescence results of major and minor elements of travertine and tufa samples.

Chemical Constituents	D3	D8	D11	D18	D23b	D26a	D26b	D 29	S1d	S10	S19
	wt %										
CaO	55.38	55.38	55.81	52.42	54.1	52.92	55.39	55.45	48.38	54.31	52.22
SiO ₂	0.22	nd	0.22	0.85	0.24	0.44	0.82	0.09	8.39	1.85	3.77
Al ₂ O ₃	0.12	0.13	0.08	0.29	0.07	0.15	0.28	0.04	1.82	0.44	0.89
TiO ₂	nd	nd	nd	0.05	nd	0.05	nd	nd	0.28	nd	0.13
Fe ₂ O ₃	0.28	1.3	0.8	2.13	3.81	0.24	0.4	0.55	4.72	0.47	1.83
MgO	0.17	0.21	0.18	0.28	0.14	0.27	0.19	0.12	0.9	0.74	0.91
MnO	nd	nd	nd	0.03	0.03	1.93	nd	0.01	0.08	0.08	0.08
Na ₂ O	nd	nd	nd	0.04	0.04	0.13	nd	0.04	0.13	0.02	0.03
K ₂ O	0.01	nd	nd	nd	nd	0.03	0.04	nd	0.85	0.08	0.23
P ₂ O ₅	dl	0.01	dl	0.02	0.01	0.01	0.01	dl	0.01	0.19	0.08
SO ₃	0.02	0.02	0.02	nd	0.01	0.07	0.02	0.01	0.03	0.11	0.08
mg/kg											
Sr	842	423	539	4189	833	3919	1200	788	511	1051	898
Zr	31	nd	nd	nd	nd	nd	nd	nd	nd	nd	nd
Mo	307	357	349	377	285	287	378	379	389	350	321
Rb	nd	nd	nd	nd	nd	nd	nd	nd	87	nd	nd
Ba	nd	447	nd	378	nd	2825	nd	nd	1035	8339	758
Cl	nd	nd	nd	nd	nd	88	nd	40	188	31	12
Br	nd	nd	nd	nd	nd	nd	nd	nd	nd	nd	nd
Chemical Constituents	S27	S32	S34	S38	S39	S45	S47b	Z1	Z1*	Z3	Z4
	wt %										
CaO	55.29	55.28	53.57	54.23	53.84	51.93	51.41	52.54	52.45	55.41	55.03
SiO ₂	0.89	1.04	1.95	1.21	1	2.01	2.81	2.03	1.24	0.81	0.82
Al ₂ O ₃	0.28	0.23	0.35	0.32	0.28	0.44	0.55	0.1	0.15	0.2	0.22
TiO ₂	nd	nd	0.08	0.05	0.09	0.08	0.11	nd	nd	nd	nd
Fe ₂ O ₃	0.83	0.47	0.87	0.91	1.81	0.53	3.43	0.88	0.18	0.17	0.47
MgO	0.42	0.9	1.03	0.82	0.89	0.79	0.92	0.54	0.74	0.47	0.85
MnO	0.03	0.04	nd	nd	0.04	0.12	0.15	2.1	0.03	nd	nd
Na ₂ O	nd	nd	0.02	0.02	0.05	0.28	0.04	1.17	0.73	nd	0.02
K ₂ O	0.05	0.05	0.08	0.05	0.04	0.1	0.18	0.1	0.11	0.04	0.05
P ₂ O ₅	dl	0.01	0.03	0.02	0.02	0.02	0.03	0.01	0.01	0.01	0.01
SO ₃	0.02	0.04	0.09	0.05	0.12	0.14	0.14	0.07	0.18	0.07	0.1
mg/kg											
Sr	588	555	1008	802	980	1811	7987	2213	897	585	837
Zr	nd	nd	nd	nd	nd	nd	nd	33	nd	nd	nd
Mo	343	234	385	410	328	373	228	378	358	308	331
Rb	nd	nd	nd	nd	nd	48	nd	nd	nd	nd	nd
Ba	547	535	8341	10,958	1019	1159	1812	nd	2955	822	1305
Cl	nd	nd	24	nd	39	23	297	877	1545	45	338
Br	nd	nd	nd	nd	nd	nd	nd	54	134	nd	nd

Z1 and Z1* are tufa samples. nd: is not detected; dl: detection limit; D: Deir Alla; S: Suwayma; Z: Az Zara.

3.2.2. Fe₂O₃ and MnO

The Fe₂O₃ content of Deir Alla samples ranges from 0.24% to 3.18% (Table 3). In Suwayma travertine, Fe₂O₃ wt % ranges from 0.47% to 4.72%, and Az Zara travertine and tufa is between 0.18% and 0.88%. Such percents are for total iron, which include the Fe precipitated with calcite and that associated with detrital minerals. According to Pentecost [8], the mean Fe wt % for the meteogene and thermogene travertines is 0.18% to 0.28%, respectively, which is far less than the mean value of the studied travertines (0.83%). This is most probably related to the presence of allochthonous Fe-minerals within the travertine.

The mean value of MnO content in Deir Alla and Suwayma travertines is about 0.14% and 0.03%, respectively, while the mean value for meteogene and thermogene travertines is 0.0188% and 0.091%, respectively [8]. MnO in Deir Alla and Suwayma travertines is most probably incorporated into calcium carbonate. The high percent of Mn in D26a sample is zoned in aragonite (Table 3). The low percent of MnO content reflects a high rate of travertine deposition in such areas [29]. Consequently, the precipitation rate in Suwayma was higher than that in Deir Alla. High percent of MnO was also recorded in Z1* tufa sample (Table 3), due to the presence of plants, especially mosses, which contain manganese in their internal structure, similar to those described by Obeidat [15]. Such MnO content indicates a slow rate of deposition of tufa [32]. Caboi et al. [33] found that Mn is mainly associated with calcite, while Fe is associated with the detrital minerals.

Pentecost [8] observed that when Fe levels are high, Mn tends to precipitate with it, but when Fe is low, Mn is incorporated into calcium carbonate. The selected travertine samples define a negative correlation between CaO and MnO (Figure 6). This might indicate that Mn is incorporated into calcium carbonate and replaces Ca.

3.2.3. Alkali Metals

The alkali metals are believed to occupy interstitial positions in the calcite lattice with a frequency of occurrence: Li > Na > K > Rb [34]. However, in aragonite, they substitute for Ca²⁺ in the crystal structure. Therefore, they are more easily co-precipitated with aragonite than with calcite [34]. It is noted that some Na concentrations in the samples are associated with Cl to form halite. In Deir Alla travertine, Na and K contents average 0.085% and 0.022%, respectively, and, similar to those found in the super-ambient travertines of Matlock Bath, UK [35]. Therefore, Deir Alla travertine is considered as super-ambient meteogene travertine, especially when the water temperature rises above ambient issuing hot springs (>37 °C) [8]. Figure 5c shows that K is correlated with Al, with a positive 0.98 correlation coefficient (Figure 6). This may indicate that they were found during the same mineral phases, such as clay minerals (potassium aluminum silicates). This is supported by the positive 0.98 correlation coefficient with SiO₂ (Figure 6).

3.2.4. Sr

The Sr content of Deir Alla samples ranges from 423 to 4189 mg/kg. In Suwayma travertine, Sr ranges from 511 to 7987 mg/kg, whereas Az Zara travertine and tufa Sr ranges from 585 to 2213 mg/kg (Table 3). The range of Sr concentration in the meteogene travertine is from 9 to >2930 mg/kg, and in the thermogene travertine is 20–14,000 mg/kg. In general, the Sr proportion in calcite is less than that in aragonite [8]. The transformation of aragonite to calcite during meteoric water circulation in depth leads to precipitation of calcite with less Sr content [8].

There is probably no single universal factor that controls calcite and aragonite precipitation in spring systems. For example, calcite was precipitated directly from waters with temperatures of >90 °C in Kenya [29] and New Zealand [36]. According to Fouke et al. [1], only aragonite precipitates at water temperatures >44 °C, whereas calcite and aragonite precipitate at 30–43 °C, while calcite alone forms when temperature falls below 30 °C. The Sr proportion increases in high-temperature travertine facies [1]. Therefore, the low temperature Deir Alla travertines have low Sr concentrations and are

commonly composed of pure calcite. Some samples that contain a high percent of Sr may reflect their high aragonite content, especially those in D26a samples that showed aragonite recrystallization under the microscope [19]. High Sr content in Suwayma travertine reflects deposition under high water temperature like aragonite, before its complete transformation into calcite. The association of aragonite and calcite in Az Zara samples indicates their formation under high water temperatures (25–45 °C), before the complete transformation of aragonite into calcite.

Kinsman [37], Veizer and Demovic [38] considered that the diagenetic solution is one of the main factors that control the distribution of Sr in the carbonate rocks. In addition, Cipriani et al. [39,40] found an appropriate correlation between Sr content and porosity, which means that calcite must contain less Sr as porosity decreases. Deir Alla travertine was affected by diagenetic processes, such as their tight lithification, high compaction, low pore spaces, and good cementation. In contrast, Suwayma travertine was affected much less by diagenetic processes, as indicated by their loose lithification, low compaction, high pore spaces, and weak cementation. A high Sr value was recorded in the Z1 sample of the spongy tufa that was slightly affected by diagenetic processes, as compared to hard travertine samples Z3 and Z4.

The negative correlation between Ca and Sr abundances in travertine samples indicates that some Ca was replaced by Sr in the calcite lattice. Ichikuni [41] observed that the partition coefficients of Sr are higher in both aragonite and calcite, if a small amount of Mn has substituted for Ca in the lattice.

3.3. Stable Isotopes

3.3.1. Background Information

The ($^{13}\text{C}/^{12}\text{C}$) and ($^{18}\text{O}/^{16}\text{O}$) ratios undergo discrete change during biogeochemical cycling, allowing inferences about their origin and past history. Such ratios provide an expanded scale for the comparative small differences observed [42]. For travertine, fractionation of carbon and oxygen isotopes is of particular interest. They provide information about the carbon dioxide source, the physio-chemical conditions of the precipitation event (rate and temperature), and the influence of metabolic processes. In favorable circumstances, they provide information about the temperature at which deposition occurred, and assist in radiometric dating [42].

Stable oxygen isotope ratios are of great interest to geochemists and carbonate sedimentologists. As the lithosphere water exchanges oxygen atoms with the dissolved carbon dioxide, and where equilibrium is established, the difference between the ratio of oxygen isotopes in carbonates and depositing water can be used to estimate past water temperatures, assuming that the fluid source has not changed through time. Information can also be obtained on rates of water evaporation with time [8,42].

The carbon stable isotopes also undergo fractionation during chemical reactions. The fractionations of $\delta^{13}\text{C}$ occur between gas phase CO_2 and the dissolved carbonate species. The CO_2 gas is slightly depleted in ^{13}C , whilst bicarbonates and carbonates are enriched by about 9% at 20 °C [8].

Carbonates have $\delta^{18}\text{O}$ (VSMOW) values ranging from about 0 to +35%. Their interpretation is generally less straightforward than carbon isotope values because carbonate oxygen readily exchanges with oxygen in water molecules [8]. Biotical and geochemical processes such as photosynthesis and temperature decrease during flow process, evaporation, mixing from soil profile or surface waters will exert an influence on the final oxygen isotope value for any carbonate sample [43,44].

3.3.2. Deir Alla Travertine

The results indicate that the $\delta^{13}\text{C}$ isotope values in the eight samples from Deir Alla are between -1.45 and 2.99 (‰ VPDB) (Table 4), while the $\delta^{18}\text{O}$ values vary from -8.13 to 8.17 (‰ VPDB). Deir Alla samples are described as super-ambient meteoene travertines [8]. The range of stable carbon isotope value in such a travertine type is from -12 to $+2$ (‰ VPDB), and the median of stable oxygen isotope is

−7.92 (‰VPDB) [8]. The bivariate distribution of $\delta^{18}\text{O}$ and $\delta^{13}\text{C}$ (‰VPDB) values in Deir Alla samples (Figure 7) shows four different travertine lithofacies that are: shrub, coated bubble, paper-raft + reed, and crystalline crust lithofacies. The stable isotope values are variable in the different sub-environments, due to possible variations in conditions (i.e., water temperature, flow velocity and distance from spring, surface area and biological effects). Figure 7 indicates that Deir Alla travertine is enriched in ^{13}C . The high $\delta^{13}\text{C}$ values in some travertine facies (as shown in D26b and D29 samples) can be explained by a combination of several processes: (i) increased CO_2 degassing processes related to travertine formation [45]; and (ii) increased input from heavier thermal-spring water ^{13}C -enriched groundwater. The cooling process of spring water during the flow tract is responsible for the loss of $\delta^{18}\text{O}$ from the water system by evaporation; as a result, the $\delta^{18}\text{O}$ value will increase. This case was observed only in the D3 sample.

Table 4. Values of $\delta^{18}\text{O}$ and $\delta^{13}\text{C}$ in the studied samples.

Sample	Facies	$\delta^{18}\text{O}$ (‰VPDB)	$\delta^{13}\text{C}$ (‰VPDB)
D3	coated bubble	8.17	1.88
D8	paper-raft + reed	−3.32	0.89
D18	Shrub	−5.48	−1.45
D23b	paper-raft + reed	−5.22	0.05
D26b	crystalline crust + palaeosol	−4.93	2.99
D29	crystalline crust	−8.13	2.83
S1d	lithoclast + pebbly	−5.1	0.89
S10	Lithoclast	−4.25	1.01
S27	Lithoclast	−5.38	0.85
S32	Lithoclast	−2.84	1.03
S38	Reed	−3.58	−0.18
S45	coated bubble	8.12	1.28
Z1	macrophyte tufa	−7.34	−2.45
Z1*	macrophyte tufa	−7.02	−1.78
Z3	coated bubble travertine	−8.83	−3.52
Z4	lithoclast + paper-raft travertine	−5.14	−1.34

VPDB: Vienna Pee Dee belemnite, standard value for C isotopes.

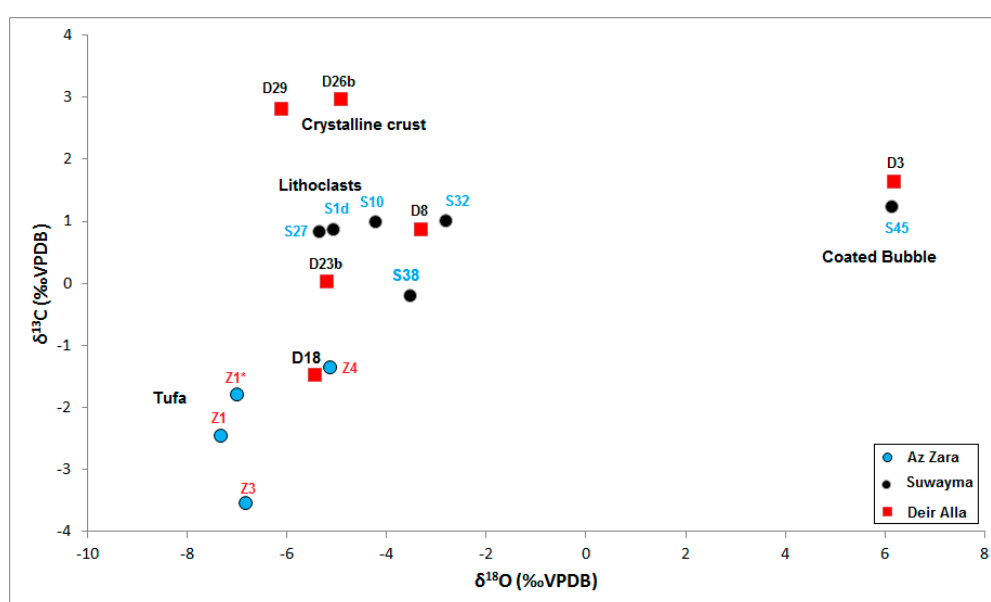


Figure 7. Bivariate plot of $\delta^{18}\text{O}$ and $\delta^{13}\text{C}$ (‰VPDB) values of the studied travertine samples.

3.3.3. Suwayma Travertine

The $\delta^{13}\text{C}$ isotope values in the six samples of Suwayma travertine vary between -0.18 and 1.28 (‰VPDB), while $\delta^{18}\text{O}$ values vary from -5.38 to 8.12 (‰VPDB) as shown in Table 4. Suwayma travertine is considered as thermogene travertine. The stable carbon isotope in such travertine type ranges from -1 to $+10$ (‰VPDB), and the median of stable oxygen isotope is -0.95 (‰VPDB) [8].

The $\delta^{18}\text{O}$ and $\delta^{13}\text{C}$ (‰VPDB) bivariate distribution of Suwayma travertines shows three different lithofacies: lithoclast, reed, and coated bubble (Figure 7). Such results explain the enrichment of $\delta^{13}\text{C}$, which depends on the depositional environment fluctuations. The $\delta^{13}\text{C}$ is likely enriched due to the increase of degassing processes that are associated with the minor microbiologic and photosynthetic activities. The occurrence of ^{13}C -enriched carbonate in the Suwayma slope indicates the presence of ^{13}C -enriched surface water and groundwater that might be washed-out during hydrological open systems. It is quite evident that the low $\delta^{18}\text{O}$ values are related to the poor evaporation effects and high water temperature during travertine formation. Additionally, the $\delta^{18}\text{O}$ depletion in the thermogene water was displayed by the isotopic exchange with the host rock [46].

3.3.4. Az Zara Tufa

The $\delta^{18}\text{O}$ and $\delta^{13}\text{C}$ values in the Az Zara tufa deposits are distinctively low compared with the other areas (Figure 7). This may indicate different isotopic signatures. The average values of carbon and oxygen stable isotopes are $-2.3\text{‰} \pm 0.2\text{‰}$ VPDB and $-8.58\text{‰} \pm 0.7\text{‰}$ VPDB, respectively.

One per mill (1%) drop in the carbonate $\delta^{18}\text{O}$ value is equivalent to about a 4.5 °C temperature rise under equilibrium conditions [8]. The $\delta^{18}\text{O}$ compositions reflect the short stagnancy time of water. The lack of evaporation or continuous recharge could be the reason in such a fluvio-palustrine depositional environment. The low $\delta^{18}\text{O}$ values may also have resulted from isotopic exchange between the circulating thermal waters and the country rock and/or water adsorbed in the clay minerals.

The occurrence of ^{13}C -poor carbonate in the Az Zara area indicates the presence of ^{13}C -poor surface and groundwater that might be washed-out when the hydrological systems are closed. The variations in $\delta^{13}\text{C}$ are minimal (-3.52‰ to -1.34‰), reflecting similar carbon sources for all facies. The carbon dioxide is believed to originate from Upper Cretaceous limestone decarbonation reaction as a result of the Karst process; however, a magmatic component may also be significant and originates from the Pleistocene basaltic activity, which is dominant within two of the studied sites (Figure 2), and probably records the influence of meteoric and soil-derived CO_2 .

3.4. Travertine Dating

3.4.1. Background Information

According to Srdoč et al. [47,48], if travertine is to be dated using ^{14}C , then the sources of carbon must be known. The ^{14}C dating method is not reliable for thermogene travertine because their carbon content is fossil (dead carbon/inorganic carbon). More reliable dates may be obtained by using a U-Series date [49,50] or by using the Electron Spin Resonance method [50]. For instance, where cosmogenic carbon is the only source, then dating is straightforward and the level of ^{14}C in the sample gives a direct measure of age [8]. The decay of isotopes ^{14}C has been used most extensively, and can date deposits up to 30 Ka. The isotope ^{14}C has a half-life of 5730 years and forms continuously in the atmosphere by the interaction of cosmic rays with molecules of nitrogen.

3.4.2. Age of Travertine

The previous studies did not provide any absolute ages of travertine in Jordan. The present work applied the radiocarbon method for dating Deir Alla and Suwayma travertines. Two rock samples were selected for radiocarbon dating. The travertine age calculations unfortunately yielded unreliable ages, and these indicate an age of 32.84 ± 0.005 Ka (Late Pleistocene).

4. Conclusions

The mineralogical compositions of the total travertine samples consist mainly of calcite with varying amounts of quartz (i.e., detrital quartz). Moreover, some aragonites are found in Deir Alla and Suwayma travertines. Based on geochemical studies, low Mg calcite is the main travertine component in all locations examined here. Accordingly, the Deir Alla travertines were classified as inactive super-ambient meteoene deposits. The Suwayma and Az Zara travertines were classified as inactive thermogene. Moreover, Az Zara tufa was classified as an active thermogene deposits.

The Sr abundances indicate pure calcite in the Deir Alla travertines and the diagenetic effect to be more than that recorded in Suwayma and Az Zara travertines. The Suwayma travertine was deposited as aragonite that completely transformed into calcite. Moreover, Az Zara travertine and tufa were deposited under high temperature water as the component of aragonite and calcite. Such aragonites are also completely transformed into calcite. The high $\delta^{13}\text{C}$ values in the travertine facies are related to evaporation effects, CO_2 degassing processes, increased input of ^{13}C -enriched groundwater, and the presence of surface and groundwater transportation medium in hydrological open systems. The high $\delta^{18}\text{O}$ values may be attributed to evaporation effects and low water temperature that prevailed during travertine formation. The travertine formed in the Late Pleistocene.

Acknowledgments: The authors thank the Deanship of Research and Graduate Studies of Hashemite University very much for funding this work through the project entitled “Genesis and palaeo-environmental significance of hot spring travertines in Jordan”. A huge thanks is due to Engineer Qais Al Qaisi, the Director of Travco Company (Amman, Jordan), who granted fieldwork access to study the travertine at the company site at Deir Alla. In addition, earnest thanks are due to Al al-Bayt University for the XRF analysis and the Water Authority for the radiogenic and stable isotope measurements. A special thanks is also extended to the anonymous reviewers of this article for their critical comments and suggestions.

Author Contributions: Khalil Ibrahim, Sana’ M. Al-Thawabteh, Issa M. Makhlof and Ali R. El Naqah conducted the field work; Sana’ M. Al-Thawabteh performed the mineral and chemical analysis; Khalil Ibrahim and Sana’ M. Al-Thawabteh analyzed the data; and Khalil Ibrahim wrote the paper.

Conflicts of Interest: The authors declare no conflict of interest.

References

1. Fouke, B.W.; Farmer, J.D.; Des Marais, D.J.; Pratt, L.; Sturchio, N.C.; Burns, P.C.; Discipulo, M.K. Depositional facies and aqueous-solid geochemistry of travertine-depositing hot springs (Angel Terrace, Mammoth Hot Springs, Yellowstone National Park, USA). *J. Sediment. Res.* **2000**, *70*, 565–585. [[CrossRef](#)]
2. Jamtveit, B.; Hammer, Ø.; Andersson, C.; Dysthe, D.K.; Heldmann, J.; Vogel, M.L. Travertines from the Troll thermal springs, Svalbard, Norway. *J. Geol.* **2006**, *86*, 387–395.
3. Fouke, B.W. Hot-spring systems geobiology: Abiotic and biotic influences on travertine formation at Mammoth hot springs, Yellowstone National Park, USA. *Sedimentology* **2011**, *58*, 170–219. [[CrossRef](#)]
4. Zhu, T.; Dittrich, M. Carbonate precipitation through microbial activities in natural environment, and their potential in biotechnology: A review. *Front. Bioeng. Biotechnol.* **2016**, *4*, 4. [[CrossRef](#)] [[PubMed](#)]
5. Capezzuoli, E.; Candin, A.; Pedley, M. Decoding tufa and travertine (fresh water carbonates) in the sedimentary record: The state of the art. *Sedimentology* **2014**, *61*, 1–21. [[CrossRef](#)]
6. Rodrigo-Naharro, J.; Delgado, A.; Herrero, M.J.; Granados, A.; Pérez del Villar, L. Current travertines precipitation from CO_2 -rich groundwaters as an alert of CO_2 leakages from a natural CO_2 storage at Gañuelas-Mazarrón Tertiary Basin (Murcia, Spain). *Inf. Técnicos Ciemat* **2013**, *1279*, 1–53.
7. Dreybrodt, W.; Buhmann, D.; Michaelis, J.; Usdowski, E. Geochemically controlled calcite precipitation by CO_2 outgassing: Field measurements of precipitation rates in comparison to theoretical predictions. *Chem. Geol.* **1992**, *97*, 285–294. [[CrossRef](#)]
8. Pentecost, A. *Travertine*, 1st ed.; Springer: London, UK, 2005; ISBN 978-1-4020-3606-4.
9. Pentecost, A.; Vile, H.A. A review and reassessment of travertine classification. *Géogr. Phys. Quat.* **1994**, *48*, 305–314. [[CrossRef](#)]

10. Alessandro, D.W.; Giammanco, S.; Bellomo, S.; Parello, F. Geochemistry and mineralogy of travertine deposits of the SW flank of Mt. Etna (Italy): Relationships with past volcanic and degassing activity. *J. Volcanol. Geotherm. Res.* **2007**, *165*, 64–70. [[CrossRef](#)]
11. Ford, T.D.; Pedley, H.M. A review of tufa and travertine deposits of the world. *Earth Sci. Rev.* **1996**, *41*, 117–175. [[CrossRef](#)]
12. Arenas, C.; Gutiérrez, F.; Osàcar, C.; Sancho, C. Sedimentology and geochemistry of fluvio-lacustrine tufa deposits controlled by evaporate solution subsidence in the central Ebro Depression, NE Spain. *Sedimentology* **2000**, *47*, 883–909. [[CrossRef](#)]
13. Jasser, D. *Investigation of Deir Alla Travertine*; Natural Resources Authority: Amman, Jordan, 1984.
14. Houry, H.; Salameh, E.; Udluft, P. On the Zerqa Ma'in (thermal kallirrhoe) travertine/Dead Sea (hydrochemistry, geochemistry and isotopic composition). *Neues Jahrb. Geol. Palaontol. Mh* **1984**, *H8*, 472–484.
15. Obeidat, O. *Geochemistry, Mineralogy, and Petrography of Travertine of Deir Alla and Zerqa Ma'in Hot Springs*. Master's Thesis, Yarmouk University, Irbid, Jordan, 1992.
16. Ibrahim, K.M.; Moh'd, B.K.; Masri, A.I.; Al-Taj, M.M.; Musleh, S.M.; Alzughoul, K.A. Volcanotectonic evolution of central Jordan: Evidence from the Shihan volcano. *J. Afr. Earth Sci.* **2014**, *100*, 541–553. [[CrossRef](#)]
17. Smit, J.; Brun, J.P.; Cloetingh, S.; Ben-Avraham, Z. The rift-like structure and asymmetry of the Dead Sea Fault. *Earth Planet. Sci. Lett.* **2010**, *290*, 74–82. [[CrossRef](#)]
18. Ferry, M.; Meghraoui, M.; Abou Karaki, N.; Al-Taj, M.; Khalil, L. Episodic behavior of the Jordan Valley section of the Dead Sea fault inferred from a 14-kyr long integrated catalogue of large earthquakes. *Bull. Seism. Soc. Am.* **2011**, *101*, 39–87. [[CrossRef](#)]
19. Al-Thawabteh, S.M. *Sedimentology, Geochemistry, and Petrographic Study of Travertine Deposits along the Eastern Side of the Jordan Valley and Dead Sea Areas*. Master's Thesis, Hashemite University, Zarqa, Jordan, 2008.
20. Salameh, E.; Bannayan, H. *Water Resources of Jordan: Present Status and Future Potentials*; Friedrich Ebert Stiftung: Amman, Jordan, 1993.
21. Salameh, E.; Udluft, P. *The Hydrodynamic Pattern of Central Jordan*; Geol Jb, C38: Hannover, Germany, 1985.
22. Water Authority of Jordan. *Open Files of the Water Authority of Jordan*; Water Authority of Jordan: Amman, Jordan, 1991.
23. Salameh, E. *Curative Water in Jordan*; WRSC Bull, 7th Issue; University of Jordan: Amman, Jordan, 1988.
24. Abu Ajamieh, M. *The Geothermal Resources of Zarqa Ma'in and Zara*; Natural Recourses Authority: Amman, Jordan, 1980.
25. Vogel, J.C. Carbon-14 dating of groundwater. In *Isotopes Hydrology*; IAEA: Vienna, Austria, 1970.
26. Thorpe, P.M.; Holyoak, D.T.; Preece, R.C.; Willing, M.J. Validity of corrected ¹⁴C dates from calcareous tufa. In *Actes Colloq. I'AGF Form. Carbonatées Externs Travertines Paris*; Springer: London, UK, 1981; pp. 151–156.
27. Greensmith, J.T. *Petrology of the Sedimentary Rocks*, 6th ed.; George Allen and UNWIN: London, UK, 1978; ISBN 0 04 552011 9.
28. Kawano, J.; Shimobayashi, N.; Miyake, A.; Kitamura, M. Precipitation diagram of calcium carbonate polymorphs: Its construction and significance. *J. Phys. Condens. Matter* **2009**, *21*, 425102–425107. [[CrossRef](#)] [[PubMed](#)]
29. Jones, B.; Renaut, R.W. Calcareous spring deposits in continental settings. In *Carbonates in Continental Settings: Facies, Environments, and Processes*; Alonso Zarza, A.M., Taner, L.H., Eds.; Elsevier Science: Amsterdam, The Netherlands, 2010; Volume 61, pp. 177–224.
30. Brian, J. Review of Calcium Carbonate Polymorph Precipitation in Spring Systems. *Sediment. Geol.* **2017**, *353*, 64–75. [[CrossRef](#)]
31. Özkul, M.; Kele, S.; Gökgöz, A.; Shen, C.C.; Jones, B.; Baykara, M.O.; Fórizs, I.; Nemeth, T.; Chang, Y.W.; Alcicek, M.C. Comparison of the Quaternary travertine sites in the Denizli Extensional Basin based on their depositional and geochemical data. *Sediment. Geol.* **2013**, *294*, 179–204. [[CrossRef](#)]
32. Rao, C.P. Petrography, trace elements and oxygen and carbon isotopes of Grodon group carbonates (Ordovician), Florentine Valley, Tasmania, Australia. *J. Sediment. Geol.* **1990**, *80*, 221–231. [[CrossRef](#)]
33. Caboi, R.; Cidu, R.; Fanfani, L.; Zuddas, P.; Zuddas, P.P. Geochemistry of Funtana Maore travertines (Central Sardinia, Italy). *Miner. Petrogr. Acta* **1991**, *34*, 77–93.

34. Okumura, M.; Kitano, Y. Coprecipitation of alkali metal ions with calcium carbonate. *Geochim. Cosmochim. Acta* **1986**, *50*, 49–58. [[CrossRef](#)]
35. Pentecost, A. The origin and development of the travertines and associated thermal waters at Matlock Bath, Derbyshire. *Proc. Geol. Assoc.* **1999**, *110*, 217–232. [[CrossRef](#)]
36. Jones, B.; Renaut, R.W.; Rosen, M.R. High-temperature (>90 °C) calcite precipitation at Waikite Hot Springs, North Island, New Zealand. *J. Geol. Soc.* **1998**, *153*, 481–498. [[CrossRef](#)]
37. Kinsman, D.J. Interpretation of Sr⁺² concentration in carbonate minerals and rocks. *J. Sediment. Pterol.* **1989**, *39*, 488–508. [[CrossRef](#)]
38. Veizer, J.; Demovic, R. Strontium as a tool in facies analysis. *J. Sediment. Pterol.* **1974**, *44*, 93–115. [[CrossRef](#)]
39. Cipriani, N.; Ercoli, A.; Malesani, P.; Vannucci, S. I travertini di Rapolano Term (Siena). *Mem. Soc. Geol. Ital.* **1972**, *11*, 31–48.
40. Cipriani, N.; Malesani, P.; Vannucci, S. I travertine dell'Italia centrale. *Boll. Serv. Geol. Ital.* **1977**, *98*, 85–115.
41. Ichikuni, M. Partition of strontium between calcite and solution: Effect of substitution by manganese. *Chem. Geol.* **1973**, *11*, 315–319. [[CrossRef](#)]
42. Sun, H.; Liu, Z. Wet-dry seasonal and spatial variations in the δ¹³C and δ¹⁸O values of the modern endogenic travertine at Baishuitai, Yunnan, SW China and their paleoclimatic and paleoenvironmental implications. *Geochim. Cosmochim. Acta* **2010**, *74*, 1018–1029. [[CrossRef](#)]
43. Chafetz, H.S.; Guidry, S.A. Bacterial shrubs, crystal shrubs, and ray-crystal crusts: Bacterially induced vs. a biotic mineral precipitation. *Sediment. Geol.* **1999**, *128*, 57–74. [[CrossRef](#)]
44. Guo, L.; Andrews, J.; Riding, R.; Dennis, P.; Dresser, Q. Possible microbial effects on stable carbon isotopes in hot-spring travertines. *J. Sediment. Res.* **1996**, *66*, 468–473. [[CrossRef](#)]
45. Turi, B. Stable isotope geochemistry of travertines. In *Handbook of Environmental Isotope Geochemistry*; Fritz, B.P., Fontes, L.J.C., Eds.; Elsevier: Amsterdam, The Netherlands, 1986; ISBN 9781483289830.
46. Fritz, P. Der Isotopengehalt der Mineralwasser von Stuttgart und Umgebung und ihrer ittel pleistozaenen Travertin-Ablagerungen. *Jber. Mitt. Oberrhein. Geol. Ver.* **1968**, *50*, 53–58.
47. Srdoč, D.; Chafetz, H.; Utech, N. Radiocarbon dating of travertine deposits, Arbuckle Mountains, Oklahoma. *Radiocarbon* **1989**, *31*, 819–828. [[CrossRef](#)]
48. Nishikawaa, O.; Furuhashia, K.; Masuyamaa, M.; Ogatab, T.; Shiraishia, T.; Shenc, C. Radiocarbon dating of residual organic matter in travertine formed along the Yumoto Fault in Oga Peninsula, northeast Japan: Implications for long-term hot spring activity under the influence of earthquakes. *Sediment. Geol.* **2012**, *243*, 181–190. [[CrossRef](#)]
49. Lovea, A.J.; Shanda, P.; Karlstromd, K.; Crosseyd, L.; Rousseau-Gueutina, P.; Priestleya, S.; Wholinge, D.; Fultonf, S.; Keppela, M. Geochemistry and travertine dating provide new insights into the hydrogeology of the Great Artesian Basin, South Australia. *Procedia Earth Planet. Sci.* **2013**, *7*, 521–524. [[CrossRef](#)]
50. Lebatard, A.; Alcicek, M.C.; Rochette, P.; Khatib, S.; Vialet, A.; Boulbes, N.; Bourles, D.L.; Demory, F.; Guipert, G.; Mayda, S.; et al. Dating the Homo erectus bearing travertine from Kocabas, (Denizli, Turkey) at least 1.1 Ma. *Earth Planet. Sci. Lett.* **2014**, *390*, 8–18. [[CrossRef](#)]

